Cambridge Centre for Computational Chemical Engineering

University of Cambridge

Department of Chemical Engineering

Preprint ISSN 1473 – 4273

Control of HCCI Combustion Phasing during Transients by Hydrogen-Rich Gas: Investigations Using a Fast Detailed-Chemistry Full-Cycle Model

Ali Aldawood, Sebastian Mosbach, Markus Kraft [1]

released: 10 March 2009

[1] Department of Chemical Engineering
University of Cambridge
Pembroke Street
Cambridge CB2 3RA
UK
E-mail: mk306@cam.ac.uk

Preprint No. 68

c4e

Key words and phrases: HCCI Combustion, Dynamic Modelling, Hydrogen Addition

Edited by
Cambridge Centre for Computational Chemical Engineering
Department of Chemical Engineering
University of Cambridge
Cambridge CB2 3RA
United Kingdom.

Fax: + 44 (0)1223 334796
E-Mail: c4e@cheng.cam.ac.uk
World Wide Web: http://www.cheng.cam.ac.uk/c4e/

Abstract

A novel modeling approach is applied to investigate the use of hydrogen-rich gas (HRG) for controlling the combustion process in a Homogenous-Charge Compression-Ignition (HCCI) engine. A detailed-chemistry stochastic reactor model is coupled with a one-dimensional gas dynamics model to account for the full engine cycle. The integrated model simulates the steady-state and transient operation of a single-cylinder HCCI engine. A previously developed tabulation scheme is utilized to speed up the detailed-chemistry simulations, which, though computationally cheap compared to many other approaches, are impractical for simulations involving a large number of cycles. A control strategy based on HRG addition is implemented using a closed-loop controller built within the gas dynamics model. Simulations conducted at different speeds and with varying loads indicate that the HRG can be effectively used to control the combustion phasing, and hence expand the operating range of the HCCI engine.

Contents

1 Introduction

The Homogeneous-charge compression-ignition (HCCI) combustion concept exhibits very attractive emissions and fuel economy characteristics. This makes it a potential alternative to current combustion modes used in internal combustion engines. Successful application of this concept, however, is still dependent on finding an effective strategy for controlling HCCI combustion mode over a wide range of operating conditions.

Many HCCI control strategies based on a dual fuel approach have been suggested and investigated in recent years. A common problem in these strategies is the need for establishing new infrastructures to supply two different fuels. For this reason, there has been a tendency to search for a dual fuel system that only needs one primary fuel to be supplied to the engine, and the secondary fuel is produced on-board by reforming part of the primary fuel. A good example of this is the case where a primary hydrocarbon fuel (such as gasoline) is used to produce hydrogen-rich gases (HRG) on-board the engine. These gases are then introduced to the engine as necessary in order to control the combustion of the primary fuel [9, 14, 16, 18, 20, 26].

The main constituent in these reformed gases is hydrogen. Other constituents include carbon monoxide, carbon dioxide and traces of light hydrocarbon gases. Typical reformer gases may have up to 80% H2 on a volumetric basis. If needed, hydrogen purity can be enhanced further through additional processing of the reformed gases (for example to suit a fuel cell based auxiliary power unit, which may require higher hydrogen purity). The HRG can be introduced into the engine cylinder along with the intake charge or with re-circulated exhaust gases, or injected directly into the cylinder. The latter case requires a dedicated injection system but it allows for a fast-response (cycle-to-cycle) combustion control.

Recent experimental work by Hosseini and Checkel [7, 8] showed that adding reformer gas to low octane and high octane primary reference fuels caused the combustion timing to retard, and consequently, the maximum combustion pressure and pressure rise rate (PRR) to decrease. Modeling work by Kongsereeparp and Checkel [10] showed the same trend when adding reformer gas to n-heptane. They observed that addition of reformer gas delays the onset of the first stage ignition and hence delays the start of combustion and decreases the rate of heat release.

However, an opposite effect was observed when HRG is added to natural gas fuelled engines [7, 8, 10, 25]. Here, the addition of hydrogen caused the start of combustion to advance rather than retard. This opposite effect was attributed to the difference in combustion characteristics between natural gas, n-heptane and primary reference fuels. The effect of HRG is dominantly thermodynamic in the case of the single-stage ignition natural gas. It was shown that addition of reformed gas alters the ratio of specific heats and increases the pre-combustion temperature causing the combustion to start earlier. In the case of two-stage ignition fuels, the effects are dominated by chemical kinetics. Addition of HRG delays the onset of the first stage ignition and hence delays the start of combustion and decreases the rate of heat release [10].

The existence of carbon monoxide was found to have a noticeable influence on the effect of hydrogen on combustion [15, 17, 19, 21, 22] [. For example, Sato et al. [15] found that

adding only hydrogen to methane caused the ignition timing to advance while adding CO caused it to retard. When a mixture of these gases is added however, the ignition timing advanced but at a slower rate than in the pure hydrogen case.

These reported effects in general indicate that hydrogen or HRG can be potentially used to control the combustion phasing in the HCCI engine. It is clear, though, that these effects are fuel specific and not universal. The purpose of this paper is to examine this potential, using a novel fast detailed-chemistry full-cycle model and utilizing a closed-loop control approach, for an HCCI engine fuelled with primary reference fuels.

Closed-loop control was used in several studies before to investigate a variety of potential control strategies. A closed-loop control strategy based on the octane number to control combustion phasing was implemented by Olsson et al. [13]. Variable compression ratio and fast thermal management were also investigated using the same approach by Haraldsson et al. [5, 6]. These three studies were conducted on an actual HCCI engine. A simple engine combustion model coupled with a closed-loop controller was used by Chang et al. [4] to investigate the potential of residual gas fraction to control the combustion timing.

The coupling of detailed chemistry and closed-loop control in the current model provides an advanced tool to investigate HCCI steady-state and transient operation over multiple cycles. This, however, comes at a price. Because of the high computational cost, extensive real-time simulations become very time consuming. To overcome this, a tabulation scheme was implemented to replace the real-time computations with pre-processed model results.

2 Model Set-Up

This study utilizes a full-cycle model to simulate steady-state and transient operation of a single-cylinder HCCI engine fuelled with primary reference fuels (mixtures of iso-octane and normal-heptane). The combustion rate and timing are controlled by varying the ratio of HRG to the base fuel.

The engine model was built using the GT-Power platform, a one-dimensional gas dynamics code capable of representing flow and heat transfer in internal combustion engines. GT-Power also contains advanced capabilities for engine operation analysis and control at both steady-state and transient conditions.

2.1 Stochastic Reactor Model

A stochastic reactor model (SRM) is coupled with the GT-Power model to account for the closed-volume portion of the engine cycle. This SRM is based on the probability density function (PDF) approach and has been used and validated in many previous studies [1–3, 11]. The SRM accounts for detailed chemical kinetics associated with combustion, as well as physical interactions such as turbulent mixing and heat transfer between the fluids and surrounding walls.

The SRM uses a ”particle” method where the physical system is represented by an en-

semble of notional particles that carry no spatial information. While the volume, density, and pressure in the cylinder are considered as global variables in the model and calculated using conventional ways, the temperature and composition evolve independently in each particle according to a probability density function (PDF). This evolution is affected by the variation in global variables, chemical reactions between different species within the particle, and turbulent mixing with other particles. Also, some particles, chosen from the ensemble according to a uniform distribution, are subjected to heat transfer with the surrounding walls. The model uses Woschni's heat transfer coefficient to account for the convective heat transfer and assumes a uniform temperature value across all surrounding walls (head, cylinder and piston). The mixing in the model occurs between particles based on proximity in temperature and composition. This method of mixing is called Euclidian Minimum Spanning Tree (EMST) and described in detail in [24].

2.1.1 Calculation of Global Variables

The instantaneous volume, $V(t)$, is calculated from the engine geometry and crank position as follows:

$$V(t) = V_c + \frac{\pi}{4}B^2(l + a - a\cos\theta - \sqrt{l^2 - a^2\cos^2\theta}) \tag{1}$$

where V_c is the clearance volume, B is the cylinder bore, l is the connecting rod length, a is the crank radius, and θ is the crank angle. The mean instantaneous density, $\rho(t)$, is defined as follows:

$$\langle\rho(t)\rangle = \frac{m}{V(t)} \tag{2}$$

where m is the total fluid mass. The pressure, $P(t)$, is calculated using the equation of state as follows:

$$P(t) = \langle\rho(t)\rangle R\frac{\langle T(t)\rangle}{\langle M\rangle} \tag{3}$$

Where R is the gas constant, $T(t)$ is the temperature and M is the molecular weight.

2.1.2 Calculation of Local Variables

As mentioned above, the variables which evolve locally in each particle are the composition, represented by mass fractions of existing chemical species, and the temperature. If the species mass fractions are denoted by $Y_1, \ldots, Y_S$, where S is the number of chemical species, and the temperature is denoted by T, then a vector ψ which represents both the composition and the temperature can be written as:

$$\psi_j = (\psi_1, \ldots, \psi_S, \psi_{S+1}) = (Y_1, \ldots, Y_S, T) \tag{4}$$

These quantities are treated as random variables and their probability density function (PDF), denoted by f, is calculated accordingly. Once the PDF is known, mean quantities can be calculated by:

$$\langle \psi_j(t) \rangle = \int \psi_j f(\psi; t) d\psi \tag{5}$$

Since the density is varying with time, it is of convenience to use the mass density function (MDF), defined as $\mathcal{F}(\psi; t) = \varrho(\psi, t) f(\psi; t)$, instead. Knowing that the integral of the probability density function (PDF) is equal to unity (i.e. $\int f(\psi; t) \mathrm{d}\psi = 1$), the integral of the mass density function will be equal to the density at any particular time, or:

$$\int \mathcal{F}(\psi; t) d\psi = \langle \varrho \rangle (t). \tag{6}$$

The time evolution of the mass density function (MDF) is calculated as follows:

$$\begin{aligned} \frac{\partial}{\partial t}\mathcal{F}(\psi;t) = & \underbrace{-\sum_{j=1}^{S+1} \frac{\partial}{\partial \psi_j}\big[G_j(\psi)\mathcal{F}(\psi;t)\big]}_{\text{Chemical kinetics term}} + \underbrace{\sum_{j=1}^{S+1} \frac{\partial}{\partial \psi_j}\Big[\mathcal{F}(\psi;t)\int \mathcal{K}(\psi;x)\mathcal{F}(x;t)dx\Big]}_{\text{Turbulent mixing term}} \\ & \underbrace{-\frac{\dot{V}}{V}\mathcal{F}(\psi;t)}_{\text{Volume change}} \underbrace{- \frac{1}{h}\big[U(\psi_{S+1}+h)\mathcal{F}(\psi_1,\ldots,\psi_S,\psi_{S+1}+h;t) - U(\psi_{S+1})\mathcal{F}(\psi;t)\big]}_{\text{Convective heat transfer}} \end{aligned} \tag{7}$$

The function $G(\psi)$ in the chemical kinetics term collectively represents the effects of chemical reactions and volume change, and is defined as follows:

$$\begin{aligned} G_j(\psi) &= \frac{M_j \dot{\omega}_j}{\rho}, \qquad j = 1, \ldots, S \\ G_{S+1}(\psi) &= -\frac{1}{c_V \rho}\sum_{i=1}^{S+1} e_i M_i \dot{\omega}_i - \frac{p}{c_V m}\frac{dV}{dt}, \end{aligned} \tag{8}$$

Here, M_j denotes the molar mass, ω_j the molar production rate, and e_i the specific internal energy of the ith species. ρ denotes the mass density, c_V the specific heat capacity at constant volume, m the total mass, and V the instantaneous cylinder volume.

The turbulent mixing term uses a mixing method in which particles to be mixed are chosen based on proximity in composition and temperature. $\mathcal{K}$ in this term collectively represents the mixing function.

The function $U(T)$ in the convective heat transfer term is defined as follows:

$$U(T) = -\frac{h_g A}{c_V m}(T - T_W), \tag{9}$$

where h_g is the Woschni's heat transfer coefficient, A is the heat transfer area, and TW is the cylinder wall temperature. The wall temperature is assumed to be uniform across all surrounding walls (i.e. internal walls of the cylinder, piston, and head).

The above PDF equation is solved using a Monte Carlo stochastic particle method. Temperature and mass fractions are calculated for each particle and then the mean values are calculated using the following approximation to Equation (5):

$$\langle \psi_j \rangle (t) = \frac{1}{N_{par}} \sum_{i=1}^{N_{par}} \psi_j^{(i)}(t) \tag{10}$$

where N_{par} is the number of stochastic particles considered in the model. More detailed description of the SRM equations and solution methodology can be found in [1–3, 11].

The SRM uses a detailed PRF chemical kinetic mechanism which contains 157 species and 1552 reactions. In order to avoid the huge computational expense associated with detailed-chemistry multi-cycle simulations, a tabulation technique was developed and implemented [12]. The technique uses the full SRM to pre-tabulate major quantities (such as ignition timing, cumulative heat release, maximum pressure rise rate, and emissions) as functions of operating variables (such as equivalence ratio, octane number, hydrogen ratio, and inlet temperature). A fast scheme is then used to retrieve and interpolate the pre-tabulated data, eliminating the need for the computationally-expensive SRM calculations.

The GT-Power model simulates the open-volume portion of the cycle and passes the closed-volume initial conditions to the SRM at the IVC point. From there, the SRM marches through the closed-volume period in pre-defined time steps until the EVO point, accounting for the compression, ignition, combustion and expansion processes in the engine cycle.

2.2 Modelled Engine

Figure 1 shows a schematic of the HCCI experimental setup used by the engine group at Sandia National Laboratories. The engine used in this setup is a six-cylinder medium-duty diesel engine converted to a single-cylinder HCCI engine. The five remaining cylinders were deactivated but kept for dynamic balancing of engine rotation. The engine is equipped with two different fuelling systems, a direct injection system and a pre-mixed fuelling system. A detailed description of the setup, which has been used extensively to study HCCI combustion, is given in [23]. The engine's main specifications are given in Table 1.

A GT-Power model of this engine was developed and calibrated. The developed model accounts only for the active cylinder and part of the intake and exhaust systems, and only considers the fully pre-mixed fuelling option (Figure 2).

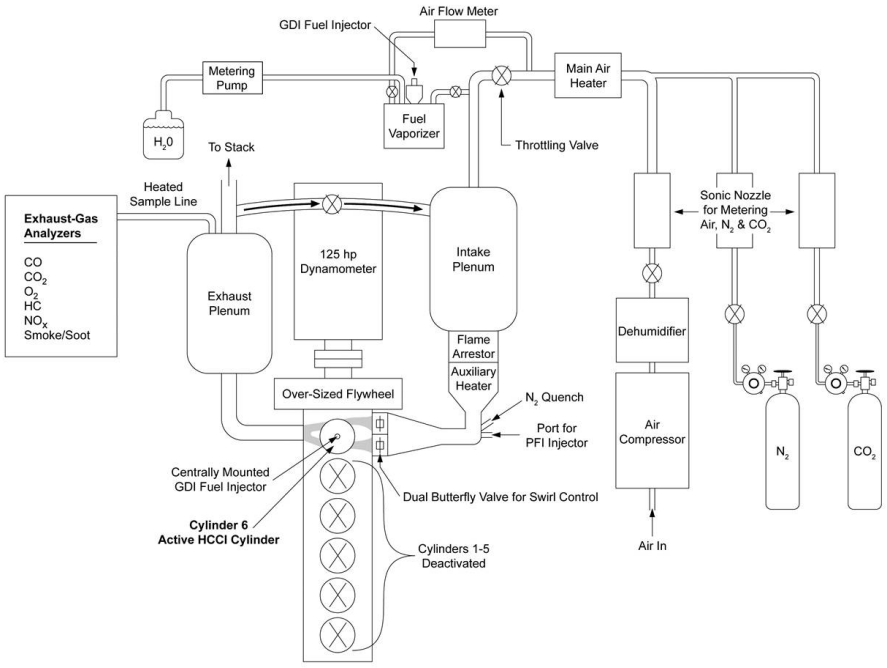

Figure 1: *A schematic of the engine setup at Sandia National Labs [23]. The single cylinder engine used in the setup is modelled in the current study.*

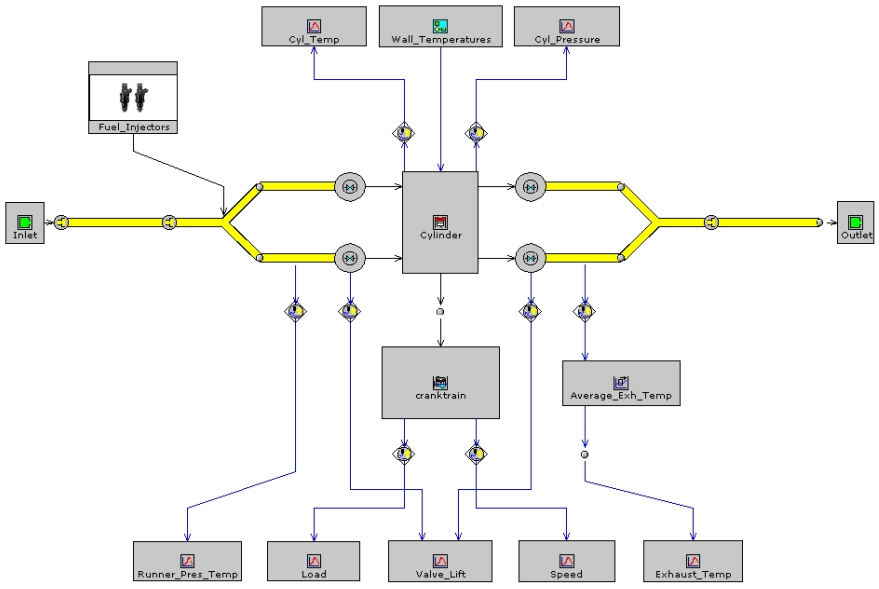

Figure 2: *A GT-Power map of the single-cylinder HCCI engine model. The GT-Power model calculates initial conditions and passes them to the SRM at IVC point.*

Table 1: *Specifications of the single-cylinder HCCI engine modeled in the current study [23].*

Parameter	Value
Cylinder displacement (liters)	0.981
Bore x Stroke (mm)	102 x 120
Connecting rod length (mm)	192
Compression ratio	13.81
Number of valves	4
IVO (CA relative to firing TDC)	357
IVC (CA relative to firing TDC)	-155
EVO (CA relative to firing TDC)	120
EVC (CA relative to firing TDC)	-352

2.3 Model Calibration

The intake pressure in the actual engine is maintained at a time-average of 1 bar by adjusting the air flow rate to the engine. Instantaneous pressure at the instant of intake valve opening (IVC) changes slightly depending on the engine speed. In the model, the pressure at the IVC changes from about 0.98 to 1.01 bar over the speed range from 600 to 2400 rpm. As in the actual engine, the exhaust pressure in the model maintained a value of 1 bar at all conditions.

In contrast to the pressure, the temperature at IVC varies significantly with engine speed. Figure 3 compares the temperature variations in the current GT-Power model with those predicted by a model developed by Sandia for the same engine [23]. The temperature readings in this case are taken 10^o CA after the bottom dead centre (BDC) during the compression stroke, which corresponds to 15^o CA before the IVC. The temperature at this instant in the cycle increases by about 20^oC as the engine speed increases from 600 to 1800 rpm. The effect of equivalence ratio on the temperature at IVC is much weaker than that of the speed and accounts only for few degrees over the whole range of equivalence ratio.

The developed GT-Power model was validated against experimental data obtained directly from Sandia or from data they published in the literature. Figure 4 shows the model results of cylinder pressure trace versus experimental results in motored operation at 1200 rpm. Exhaust temperatures at various speeds in motored operation are also compared in Figure 5.

Performance of the coupled GT-Power/SRM model at fired operation was also validated against a set of experimental data obtained from Sandia. Figure 6 compares the cylinder pressure trace as predicted by the model to experimental results at equivalence ratio of Φ=0.44 and engine speed of 1200 rpm. Both the engine and the model use a fuel comprised of iso-octane and normal-heptane only. The shown fit was obtained with a model octane number of 62 as opposed to 83 in the experiment.

The results show that the model does not predict the low temperature reactions properly. This and the discrepancy in octane number can be mainly attributed to the deficiency in

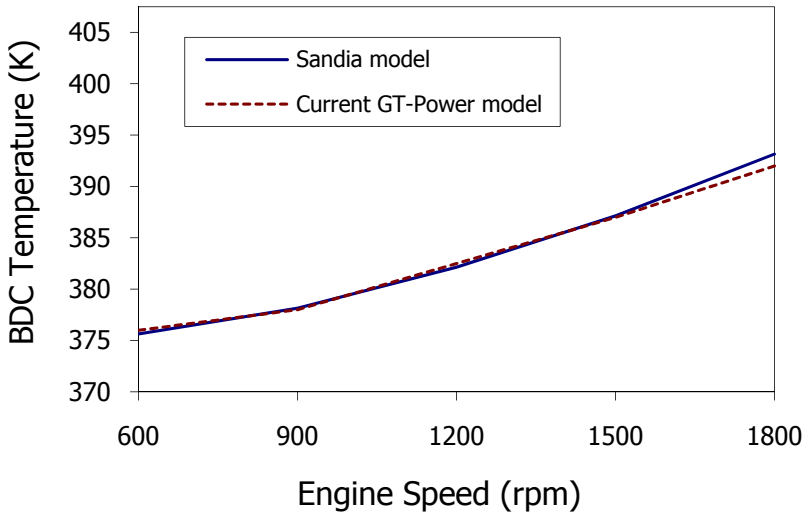

Figure 3: *Comparison of cylinder temperature at 10o after BDC in the compression stroke as predicted by Sandia's model [23] and current GT-Power model at motored operation.*

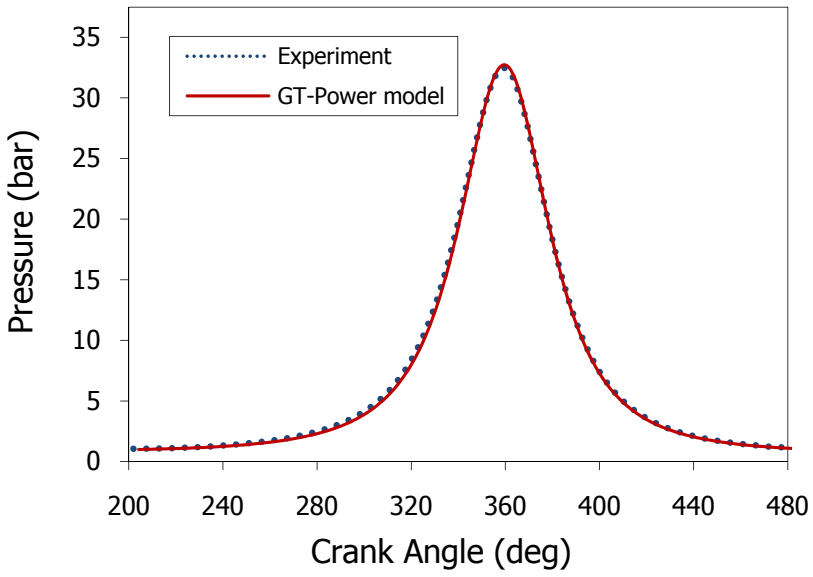

Figure 4: *Model validation against experimental data of motored operation at an engine speed of 1200 rpm.*

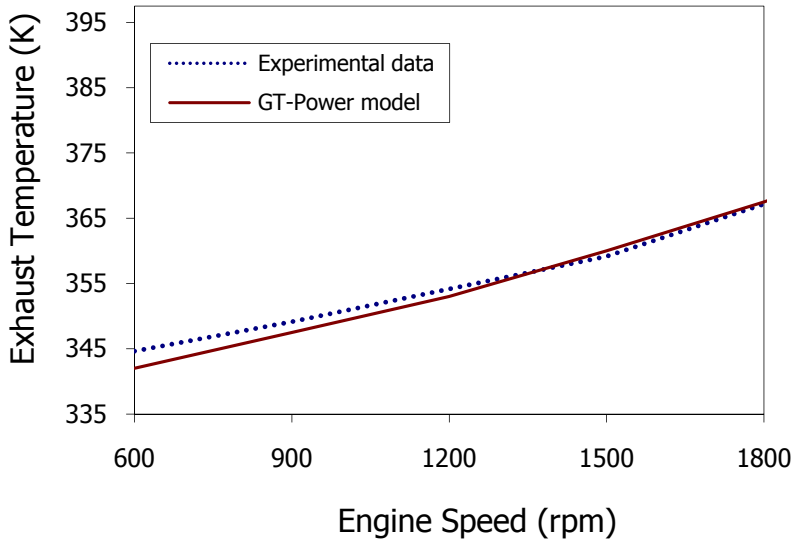

Figure 5: *Exhaust temperature versus engine speed as predicted by the GT-Power model compared to experimental readings at motored operation.*

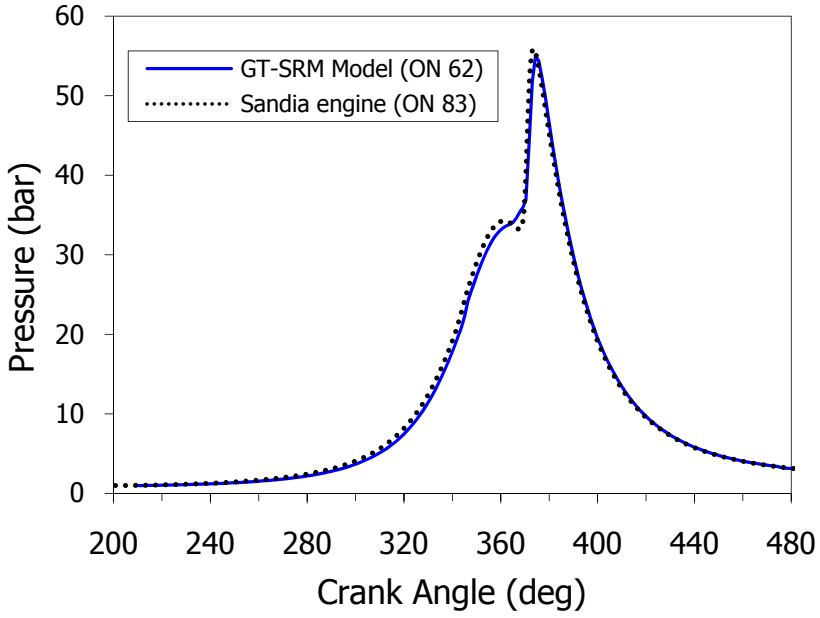

Figure 6: *Model validation of fired operation at an engine speed of 1200 rpm and equivalence ratio (Φ) of 0.44.*

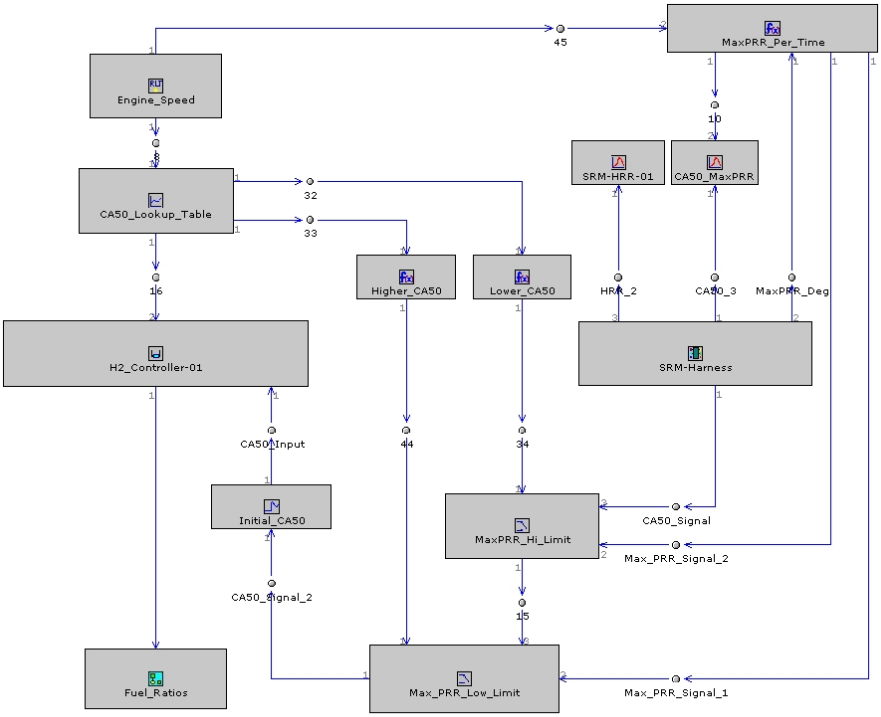

Figure 7: *A GT-Power map of the PID-based combustion phasing controller. The controller varies the HRG ratio to adjust the CA50 and keeps the pressure rise rate within acceptable range.*

the chemical kinetic mechanisms employed in the model. Also, the fact that the SRM in the current setup does not account for residual gases (i.e. gases left out from previous cycle) is another possible source of these discrepancies. Residual gases usually contain traces of active species that enhance low temperature reactions and hence affect ignition timing and pressure rise rate. Using a lower octane number fuel (which contains more normal-heptane) compensates for the lack of these active species.

2.4 Controller

The strategy is implemented using a PID-based closed-loop controller which adjusts the combustion phasing by varying the ratio of HRG to the base fuel. Figure 7 shows the GT-Power map for this PID controller.

The combustion phasing reference point considered here is CA50, the crank angle at which 50% of heat has been released. The CA50 is calculated by the SRM upon the end of each cycle and passed to the PID controller which uses it to determine the necessary change in HRG ratio. This change is implemented by the SRM in the following cycle. The SRM also passes pressure rise rate (PRR) information to the controller to indicate whether the cycle is operating in the normal, knocking, or misfiring region. High PRR indicate that the cycle is operating at or beyond the knocking boundary of the operating window, and low values indicate that the cycle is operating at or beyond the misfiring

boundary. Based on the PRR information, the controller makes adjustments to keep the next cycle within the normal region. A PRR threshold of 20 bar/ms is used to mark the misfire limit, and 80 bar/ms to mark the knock limit. This range corresponds to about 2-7 bar/degree at 1200 rpm. The upper limit was adopted based on information obtained from Sandia, and the lower limit was selected based on analysis of our simulations.

3 Results

Simulations of transient load conditions were carried out at three different speeds: 1200, 1500, and 1800 rpm. The base fuel used in these simulations has an octane number of 40 (this number, of course, will correspond to a higher octane number in the actual experiment, given the lower reactivity exhibited by the chemical model). The applied HRG is composed mainly of hydrogen with only a small volumetric portion of carbon monoxide (about 2.3% CO on volume basis and 25% on mass basis). The temperature of the intake air was 55^{o}C (328 K). A fixed combustion phasing angle (CA50) of 8 degrees after TDC was used in all simulation runs.

Figure 8 shows the simulation results for 1200 rpm. Equivalence ratio was increased (in steps of 0.01) from 0.3 to 0.52. The equivalence ratio here accounts for the added HRG as well as the base fuel. With no control in place, CA50 continued to advance with the increase in load, causing the pressure rise rate to increase. The knock limit was soon reached.

With the controller activated, the combustion phasing was effectively stabilized around the target angle during most of the run, and most importantly, the pressure rise rate was kept within the acceptable range. This extended the HCCI operation to the whole run. At the maximum load in this run, the HRG ratio was about 14

Similar effects were observed at 1500 and 1800 rpm engine speeds (Figure 9 and Figure 10, respectively). The HRG addition was quite effective in maintaining the combustion phasing and pressure rise rate even at high speed, high load conditions. Unstable operation of the controller is observed towards the end of the 1800 rpm run. The controller doesn't seem capable of adjusting the CA50 at these conditions to the chosen target value. This may have resulted from the rapid pressure rise rate at these conditions, or may simply indicate improper controller tuning.

The results from these simulations also indicate that HRG control is not suitable for very low loads. At these conditions, the engine is already operating at or close to the misfire limit with a very low pressure rise rate. A combustion enhancement strategy, such as intake temperature heating, is needed to maintain the operation above the misfire limit.

4 Conclusion

A control strategy for HCCI combustion phasing based on hydrogen-rich gas addition was presented in this paper. The results were based on a modeling study which utilized a detailed-chemistry full-cycle model to simulate steady-state and transient operation of

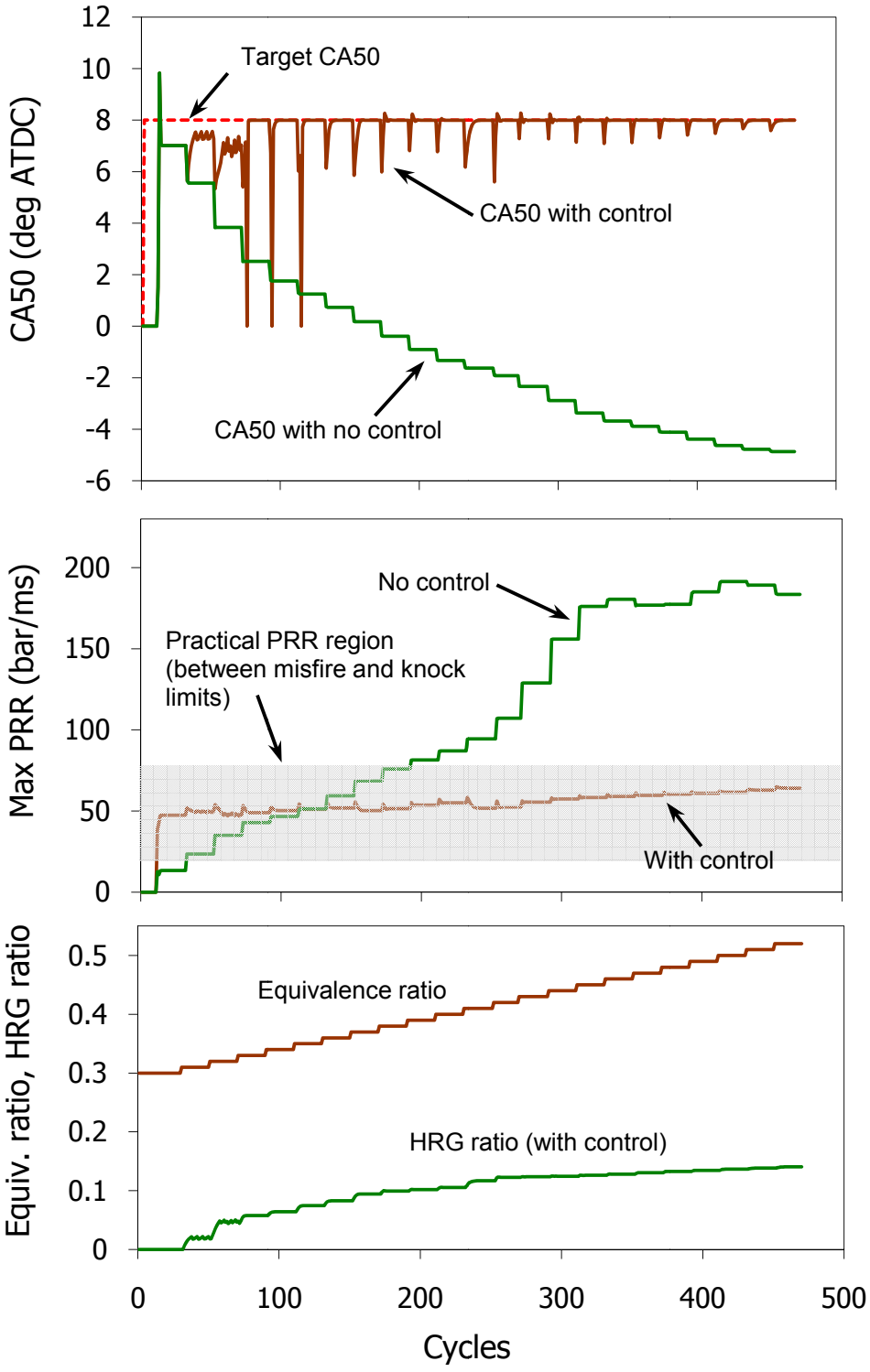

Figure 8: *Combustion phasing control during load increase and at engine speed of 1200 rpm. CA50 is stabilized around the target value, and pressure rise rate is kept within limits throughout the run.*

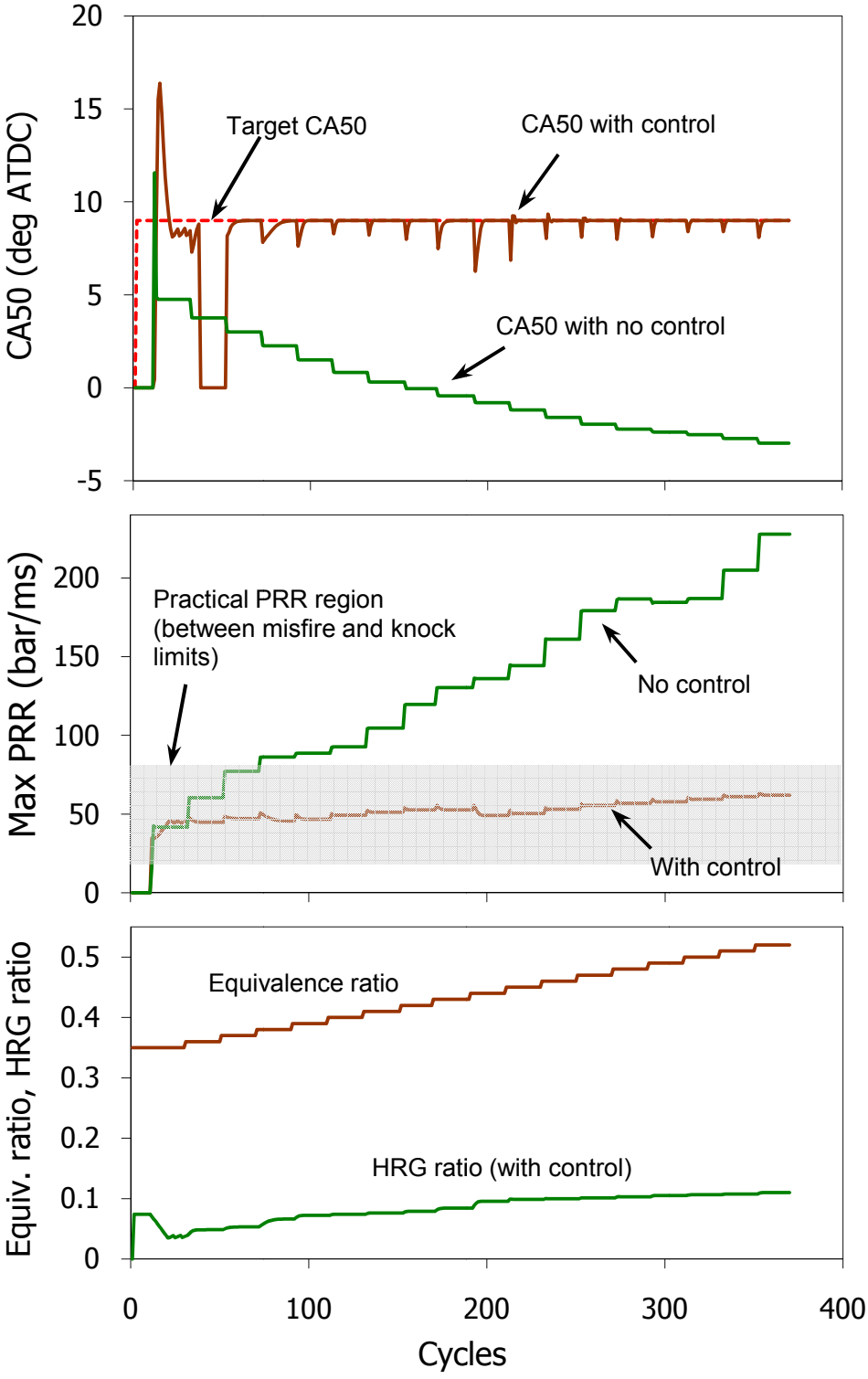

Figure 9: *Combustion phasing control during load increase and at engine speed of 1500 rpm. The operating range in the non-controlled case is very limited. Addition of HRG extended the operation to the end of the run.*

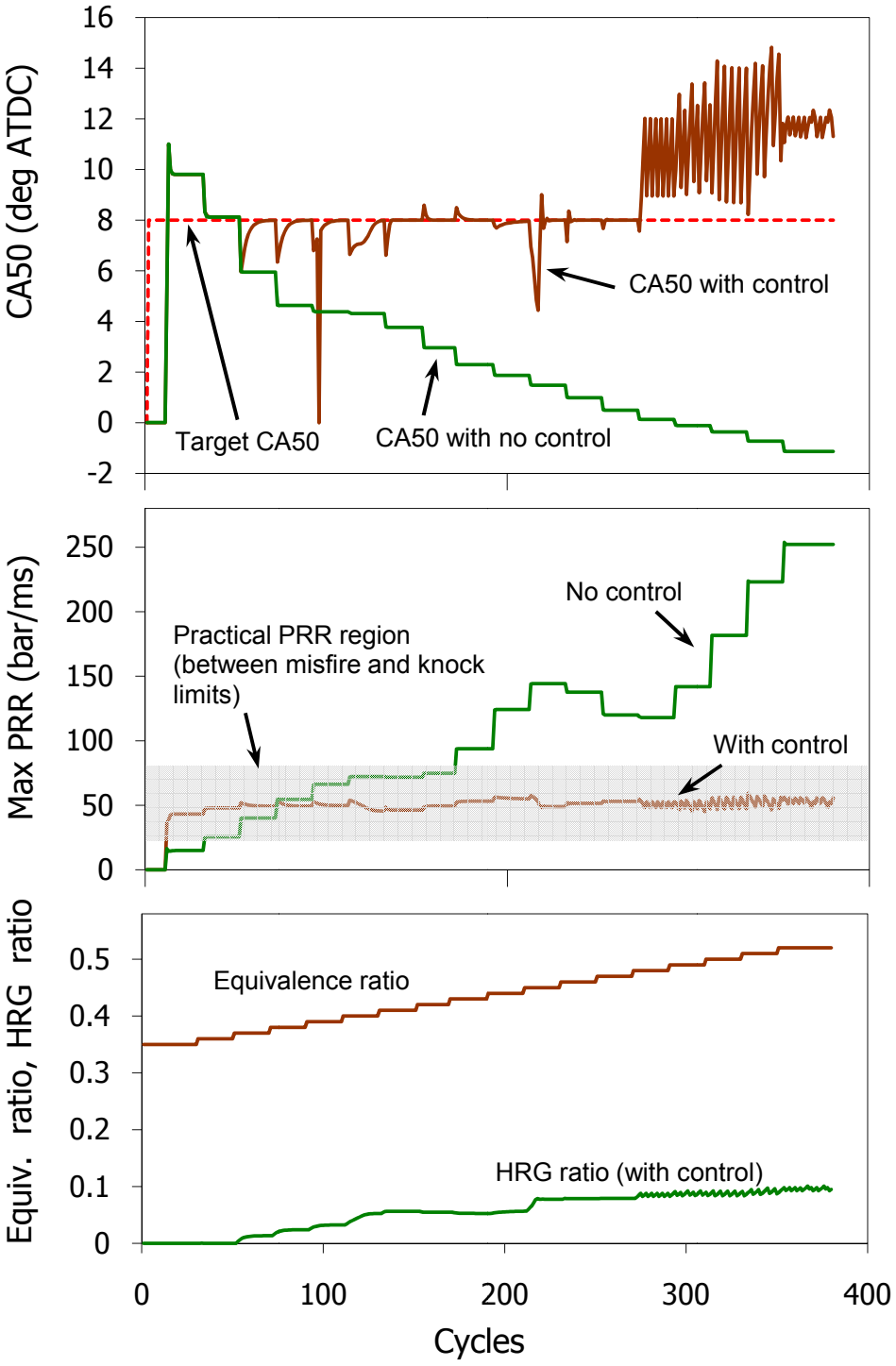

Figure 10: *Combustion phasing control during load increase and at engine speed of 1800 rpm. CA50 is stabilized around the target value except for the later part of the run where the operation of the controller becomes unstable.*

a single-cylinder HCCI engine fuelled with primary reference fuels. A tabulation scheme was implemented to speed-up the computationally expensive detailed-chemistry simulations. Simulations at different operating conditions suggested that moderate ratios of hydrogen-rich gas can be used effectively to control the combustion phasing in the HCCI engine, and extend its operating range significantly. However, control based only on hydrogen-rich gas may not be suitable at very low loads.

5 Acknowledgement

This work was primarily funded by Aramco Overseas Company B.V., contract number 6600014846, under the title "Modeling of Petrol Fuel Combustion in HCCI". Partial funding was also provided by EPSRC under the grant number EP/D068703/1. The authors would like to thank Magnus Sjöberg and John Dec of Sandia National Laboratories for providing the experimental data.

6 Definitions, Acronyms and Abbreviations

BDC	Bottom dead centre
CA	Crank angle
CA50	Crank angle at 50 percent heat release
EVO	Exhaust valve opening
HCCI	Homogeneous charge compression ignition
HRG	Hydrogen-rich gas
IVC	Intake valve closure
IVO	Intake valve opening
PID	Proportional, integral, and differential
PRF	Primary reference fuel
PRR	Pressure rise rate
rpm	Revolutions per minute
SRM	Stochastic reactor model
TDC	Top dead centre

References

[1] A. Bhave, M. Balthasar, M. Kraft, and F. Mauss. Analysis of a natural gas fuelled homogeneous charge compression ignition engine with exhaust gas recirculation using a stochastic reactor model. *International Journal of Engine Research*, 5(1), 2004.

[2] A. Bhave, M. Kraft, L. Montorsi, and F. Mauss. Modelling a dual-fuelled multi-cylinder HCCI engine using a PDF based engine cycle simulator. *SAE Paper No. 2004-01-0561*, 2004.

[3] A. Bhave, M. Kraft, F. Mauss, A. Oakley, and H. Zhao. Evaluating the EGR-AFR operating range of a HCCI engine. *SAE Paper No. 2005-01-0161*, 2005.

[4] K. Chang, G. Lavoie, A. Babajimopoulos, Z. Filipi, and D. Assanis. Control of multi-cylinder HCCI engine during transient operation by modulating residual gas fraction to compensate for wall temperature effects. *SAE Paper No. 2007-01-0204*, 2007.

[5] G. Haraldsson, P. Tunestål, and B. Johansson. HCCI combustion phasing with closed-loop combustion control using variable compression ratio in a multi cylinder engine. *SAE Paper No. 2003-01-1830*, 2003.

[6] G. Haraldsson, P. Tunestål, and B. Johansson. HCCI closed-loop combustion control using fast thermal management. *SAE Paper No. 2004-01-0943*, 2004.

[7] V. Hosseini and M. Checkel. Effect of reformer gas on HCCI combustion - Part I: High octane fuels. *SAE Paper No. 2007-01-0208*, 2007.

[8] V. Hosseini and M. Checkel. Effect of reformer gas on HCCI combustion - Part II: Low octane fuels. *SAE Paper No. 2007-01-0206*, 2007.

[9] Y. Jamal and M. Wyszynski. On-board generation of hydrogen-rich gaseous fuels: A review. *International Journal of Hydrogen Energy*, 19(7), 1994.

[10] P. Kongsereeparp and D. Checkel. Investigating the effects of reformed fuel blending in a methane or n-heptane HCCI engine using a multi-zone model. *SAE Paper No. 2007-01-0205*, 2007.

[11] S. Mosbach, M. Kraft, A. B. F. Mauss, J. Mack, and R. Dibble. Simulating a homogenous charge compression ignition engine fuelled with a DEE/EtOH blend. *SAE Paper No. 2006-01-1362*, 2006.

[12] S. Mosbach, A. Aldawood, and M. Kraft. Real-time evaluation of a detailed chemistry HCCI engine model using a tabulation technique. *Combustion Science and Technology*, 180(7), 2008.

[13] J. Olsson, P. Tunestål, and B. Johansson. Closed-loop control of an HCCI engine. *SAE Paper No. 2001-01-1031*, 2001.

[14] S. Peucheret, M. Wyszynski, R. Lehrle, S. Golunski, and H. Xuc. Use of catalytic reforming to aid natural gas HCCI combustion in engines: Experimental and modeling results of open-loop fuel reforming. *International Journal of Hydrogen Energy*, 30, 2005.

[15] S. Sato, Y. Yamasaki, H. Kawamura, and N. Iida. Research on the influence of hydrogen and carbon monoxide on methane HCCI combustion. *JSME International Journal*, 48(4), 2005.

[16] T. Shudo. An HCCI combustion engine system using on-board reformed gases of methanol with waste heat recovery: Ignition control by hydrogen. *International Journal of Vehicle Design*, 41, 2006.

[17] T. Shudo and Y. Ono. HCCI combustion of hydrogen, carbon monoxide and dimethyl ether. *SAE Paper No. 2002-01-0112*, 2002.

[18] T. Shudo and Y. Ono. Ignition control by DME-reformed gas in HCCI combustion of DME. *SAE Paper No. 2003-01-1824*, 2003.

[19] T. Shudo and T. Takahashi. Influence of reformed gas composition on HCCI combustion of onboard methanol-reformed gases. *SAE Paper No. 2004-01-1908*, 2004.

[20] T. Shudo and H. Yamada. Hydrogen as an ignition-controlling agent for HCCI combustion engine by suppressing the low-temperature oxidation. *International Journal of Hydrogen Energy*, 32(14), 2007.

[21] T. Shudo, Y. Ono, and T. Takahashi. Influence of hydrogen and carbon monoxide on HCCI combustion of dimethyl ether. *SAE Paper No. 2002-01-2828*, 2002.

[22] T. Shudo, S. Kitahara, and H. Ogawa. Influence of carbon dioxide on combustion in an HCCI engine with the ignition-control by hydrogen. *SAE Paper No. 2006-01-3248*, 2006.

[23] M. Sjöberg and J. Dec. An investigation of the relationship between measured intake temperature, BDC temperature, and combustion phasing for premixed and DI HCCI engines. *SAE Paper No. 2004-01-1900*, 2004.

[24] S. Subramaniam and S. Pope. A mixing model for turbulent reactive flows based on euclidean minimum spanning trees. *Combustion and Flame*, 115, 1998.

[25] D. Yap, A. Megaritis, S. Peucheret, M. Wyszynski, and H. Xu. Effect of hydrogen addition on natural gas HCCI combustion. *SAE Paper No. 2004-01-1972*, 2004.

[26] D. Yap, S. Peucheret, A. Megaritis, M. Wyszynski, and H. Xu. Natural gas HCCI engine operation with exhaust gas fuel reforming. *International Journal of Hydrogen Energy*, 31, 2006.